Decrease in negative ion mobility with increasing H_2O concentration in O_2

Y. Okuyama[1], K. Arai[1], S. Suzuki[1], H. Itoh[1]

[1] *Chiba Institute of Technology, Department of Electrical, Electronics and Computer Engineering, Tsudanuma, Narashino, Chiba, 275-0016, Japan*

The mobility of negative ions in O_2 was measured while varying the H_2O concentration using a high-pressure ion drift tube with a point plane gap acting as a negative ion detector. The H_2O concentration was monitored during the mobility measurement with a trace moisture analyser whose operation was based on a photoabsorption method. First, a constant mobility of 2.39 $cm^2/V{\cdot}s$ was observed in ultrahigh-purity O_2 (99.99995%, purified with a gas purifier), in which the H_2O concentration was monitored to be between 15 and 100 ppb. This mobility was concluded to be that of O_4^-. Then, a small amount of H_2O from 3500 to 17000 ppb was added to the ultrahigh-purity O_2. With increasing H_2O concentration, ion mobilities of 2.31 and 2.21 $cm^2/V{\cdot}s$ were observed in H_2O concentration ranges of 3500 - 4600 and 4600 - 17000 ppb, respectively. These mobilities are considered to be those of $O_2^-{\cdot}(H_2O)_n$. Thus, we obtained a decrease in the negative ion mobility with increasing H_2O concentration in O_2.

1. Introduction

A large amount of ion mobility data was reported in the 20th century as fundamental data for discharge plasmas [1], which has been summarized in databases [2, 3].

Most of the ion mobility measurements in O_2 have been carried out at pressures of below atmospheric pressure. One of the reasons for this is that a mass spectrometer is necessary to identify the ion species. Snuggs et al. [4], McKnight [5] and Harrison and Moruzzi [6] measured negative ion mobilities at pressure of lower than 10 Torr using a mass spectrometer and identified the ion species. Thus, obtained mobilities of O^-, O_2^- and O_3^- in O_2 have been summarized in a database as 3.20, 2.17 and 2.55 $cm^2/V{\cdot}s$, respectively, [2].

Recently, ion mobility measurement has been carried out at high pressures. Urquijo et al. [7] reported the negative ion mobility in O_2 at relatively high pressures of 100 to 600 Torr. Sabo et al. [8] performed ion mobility measurement in O_2 at atmospheric pressure in a setup including a mass spectrometer.

Meanwhile, ion mobility spectrometry (IMS) and ion mobility spectrometry / mass spectrometry (IMS/MS) have been developed for a wide range of applications under atmospheric pressure such as the detection of trace amounts of gases, explosives and drugs [9-11]. Thus, ion mobility data at high pressures are required in these fields.

In our laboratory, we have measured the negative ion mobility in O_2 at high pressures including atmospheric pressure [12-14]. We consider that the effects of impurities are difficult to avoid in ion mobility measurement such as those contained in a gas cylinder or outgassed from the surface of a chamber. Therefore, the negative ion mobility was measured in ultrahigh-purity O_2 of 99.99995% purity (Taiyo Nippon Sanso Co., Ltd.) with a gas purifier (MICROTORR: MC200-203FV). A constant negative ion mobility of 2.39 $cm^2/V{\cdot}s$ was observed in the range of a reduced electric field E/N of $2.83 \times 10^{-2} \leq E/N \leq 5.31$ Td [12, 13]. In contrast, a constant mobility of 2.31 $cm^2/V{\cdot}s$ was obtained in high-purity O_2 of 99.9999% purity [13, 14]. The reason for the difference is considered to be the concentration of H_2O in the O_2. In ultrahigh-purity O_2, the H_2O concentration was 15 - 100 ppb compared with 500 ppb as the nominal value for high-purity O_2 [12]. Thus, we considered that the ion mobility of O_4^- was observed in the former case, whereas that of $O_2^-{\cdot}(H_2O)$ was observed in the latter case.

2. Experimental setup

Figure 1 shows a cross section of the ion drift tube and a schematic diagram of the measurement system used in this study. The method used for measuring the negative ion mobility has already been described in previous papers [13, 14]. An ion drift tube with a positive corona gap is attached to a flange by supporting posts S and base plate B. G_1 is the ion drift space, which is composed of anode A, and cathode C and 10 guard ring electrodes D. G_2 is a positive corona gap composed of anode A and point electrode P which acts as an ion detector. At the center of anode A is mesh electrode M which is a 200-mesh electrode made of stainless steel wires with 0.05 mm diameter whereas cathode C is made of brass. The surfaces of electrodes C and M are covered with gold plating. Electrons are emitted from the surfaces of electrodes

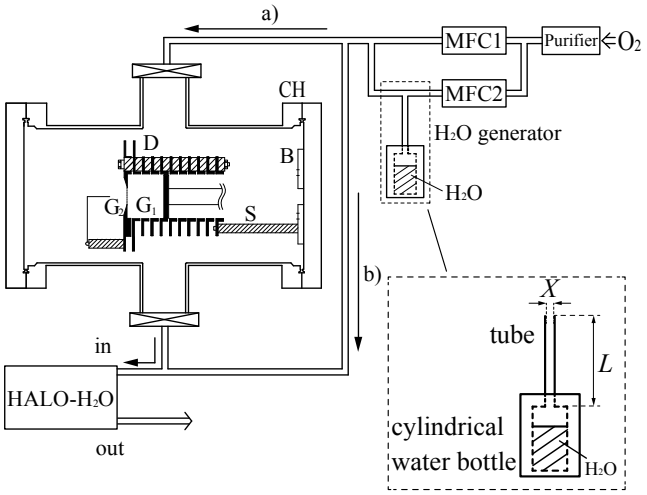

Figure 1 Cross section of ion drift tube and schematic diagram of the measurement system

C and M by irradiation with pulsed UV light generated by a spark discharge between the spherical electrodes in air. Thus, negative ions are formed by the attachment of electrons to O_2. We used ultrahigh-purity O_2 of 99.99995% purity (Taiyo Nippon Sanso Co., Ltd.) with a gas purifier (MICROTORR: MC200-203FV) that can reduce the concentrations of H_2O and CO_2 to less than 100 ppt. Moreover, a small amount of H_2O vapor was added to the ultrahigh-purity O_2 through a H_2O generator to vary the H_2O concentration in O_2. Ultrahigh-purity O_2 leaving the gas purifier gasses through mass flow controllers MFC1 and MFC2 and the H_2O generator. The H_2O concentration can be varied by adjusting the gas flow rate through MFC1 and MFC2. After the mass flow controllers, the gas line was separates into two paths. One path flows directly to the chamber (CH, figure 1 a)), and the other path flows to a bypass (figure 1 b)).

A schematic diagram of the generator used to form trace amounts of H_2O is also shown in the same figure. A cylindrical water bottle is filled with purified H_2O. A certain amount of H_2O vapor is evaporated from the outlet of a tube attached to the top of the cylindrical water bottle where the amount of H_2O depends on the length L and inner diameter X of the tube [15]. Thus, the trace amount of H_2O is diluted with ultrahigh-purity O_2.

The H_2O concentration during the measurement was monitored by a trace moisture analyzer (HALO-H_2O) whose operation principle was based on cavity ring-down spectroscopy (CRDS) [16]. H_2O concentrations can be monitored from 2 to 20000 ppb. Without the mass flow controllers and H_2O generator, the lowest concentration of H_2O through passing the bypass was measured to be 2 ppb, which is the lowest value that can be monitored by HALO-H_2O.

The impurities contained in the O_2 including observed H_2O concentration monitored by HALO-H_2O are listed in Table 1, where the concentrations of the impurities with the exception of H_2O are nominal values. The fluctuation of the H_2O concentration monitored by HALO-H_2O was ± 10% as described in detail in section 3. To avoid the effect of the impurities, the CH, HALO-H_2O and all gas lines were evacuated by a pump and the CH was heated to 100 ºC between each measurement.

Table 1 Impurities contained in O_2

Impurities	Ultrahigh-purity O_2	Ultrahigh-purity O_2 with H_2O
N_2	< 0.2 ppm	< 0.2 ppm
CO	< 0.02 ppm	< 0.02 ppm
CO_2	< 0.1 ppb	< 0.1 ppb
Ar	< 0.05 ppm	< 0.05 ppm
THC	< 0.02 ppm	< 0.02 ppm
H_2O	0.015 ~ 0.1 ppm	5 ~ 17 ppm

3. Experimental results

3.1. Negative ion mobility and H_2O concentration

Figure 2 shows the observed negative ion mobility and H_2O concentration. Figure 2(a) shows the results of the measurement carried out in ultrahigh-purity O_2. In this measurement, MFC1, MFC2 and the H_2O generator were detached from the system, i.e., ultrahigh-purity O_2 flowed to the CH directly. A purge meter was attached to the outlet of HALO-H_2O to control the flow rate of O_2 to 0.5 l/min. The measurement was carried out with E/N = 1.5 Td, p_0 = 850 Torr and an ion drift gap of d = 3 cm. A constant value of 2.39 $cm^2/V{\cdot}s$ was observed which was attributed to the ion mobility of O_4^- [12, 13]. The H_2O concentration monitored by HALO-H_2O was taken to be a constant value of 17 ppb during the measurement.

Figure 2 b) shows the result of adding H_2O to the ultrahigh-purity O_2 using the H_2O generator. In this measurement, the flow rate of MFC1 was 0.65 l/min and that of MFC2 was zero. The H_2O concentration was increased to 3900 ppb compared with 17 ppb in ultrahigh-purity O_2, The gas pressure p_0 in the CH was observed to be 900 Torr. It was found that the negative ion mobility decreased to 2.31 $cm^2/V{\cdot}s$ in agreement with the mobility obtained in high-purity O_2 with a nominal H_2O concentration of less than 0.5 ppm [13, 14].

Figure 2 c) shows the result of increasing the H_2O concentration to 8000 ppb while decreasing of the flow rate of MFC1 from 0.65 to 0.5 l/min. In this measurement, the gas pressure p_0 was 850 Torr. A new value of 2.21 $cm^2/V{\cdot}s$ was observed in the case

of E/N = 1.5 Td in good agreement with the value of 2.23 $cm^2/V{\cdot}s$ for O_4^- reported by Urquijo et al. [7].

Figure 3 shows the negative ion mobility and H_2O concentration plotted against E/N. Three different values of the negative ion mobility were obtained for different H_2O concentration ranges in O_2. A constant mobility of 2.39 $cm^2/V{\cdot}s$ regardless of the value of E/N was observed between H_2O concentrations of 15 and 100 ppb (Figure 3 a)) and constant mobilities of 2.31 and 2.21 $cm^2/V{\cdot}s$ were obtained also regardless

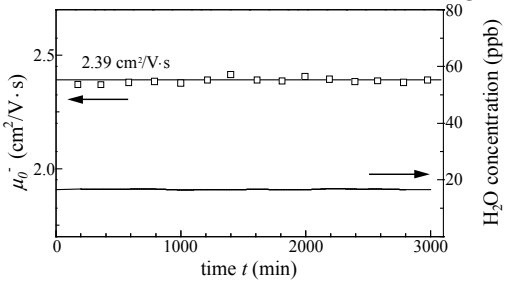

a) in ultrahigh-purity O_2 (17 ppb)

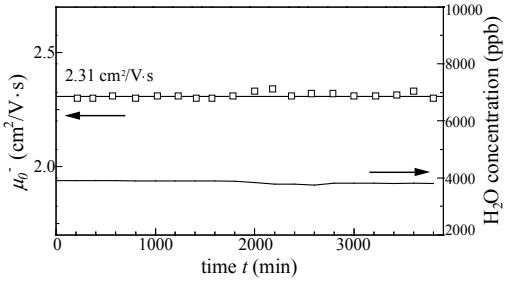

b) in O_2 added with H_2O (3900 ppb)

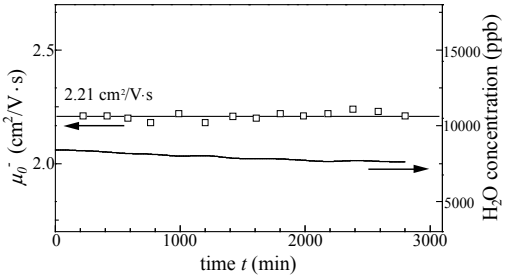

c) in O_2 added with H_2O (8000 ppb)

Figure 2 Negative ion mobility and H_2O concentration

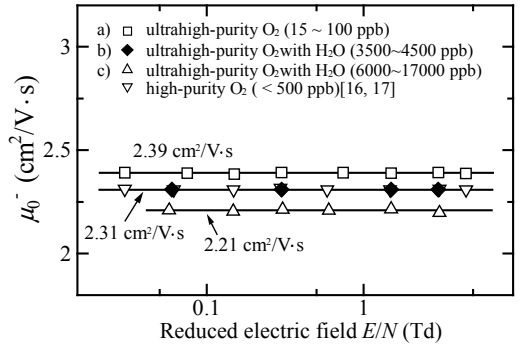

Figure 3 Negative ion mobility depended on H_2O concentration a) b) and c) against E/N

of E/N between H_2O concentrations of 3500 and 4500 ppb (Figure 3b)) and 6000 and 17000 ppb (Figure 3 c)), respectively. Thus, it is considered that the negative ion mobility decreased with increasing H_2O concentration.

Note that the H_2O concentration in ultrahigh-purity O_2 could be reduced to less than 100 ppt using the gas purifier. We observed H_2O concentrations of between 15 and 100 ppb in the range of H_2O concentration during the mobility measurement. This is considered to be because H_2O was released from the inner surface of the CH, drift tube and piping.

To summarize, the negative ion mobility was measured at H_2O concentrations of 15 - 100 and 3500 - 17000 ppb in ultrahigh-purity O_2 and ultrahigh-purity O_2 with H_2O, respectively.

3.2. Variation of negative ion mobility with H_2O concentration

Figure 4 shows the variation of the negative ion mobility with the H_2O concentration in O_2 at E/N = 1.5 Td. A stepwise decrease in the negative ion mobility which took values of 2.39, 2.31 and 2.21 $cm^2/V{\cdot}s$ was observed with increasing of H_2O concentration in the ranges of 15 - 100, 3500 - 4600 and 4600 - 17000 ppb, respectively. The reason for the decreased mobility is considered to be the formation of $O_2^-{\cdot}(H_2O)_n$ (n = 1, 2, 3…), i.e., the ion mobility decreases with increasing cluster size n.

The stepwise change in the mobility from 2.31 to 2.21 $cm^2/V{\cdot}s$ occurred at a H_2O concentration of about 5000 ppb, whereas that from 2.39 to 2.31 $cm^2/V{\cdot}s$ occurred at a concentration between 100 and 3500 ppb. These results suggest that the dominant ions are O_4^- and $O_2^-{\cdot}(H_2O)_n$ (n = 1, 2, 3…), whose mobility depends on the H_2O concentration in O_2 as shown in Figure 4. Unfortunately, the negative ion mobility is not yet clear between H_2O concentrations of 100 and 3500 ppb. Note that the gas pressures p_0 depended on the flow rate and the measurement was

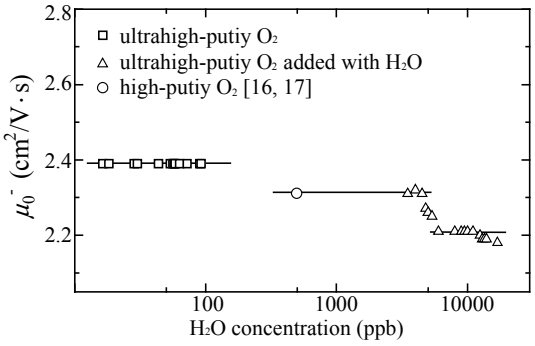

Figure 4 Variation of negative ion mobility with H_2O concentration in O_2

carried out at pressures varying between 850 and 950 Torr.

Figure 5 shows histograms of the observed mobility plotted against the H_2O concentration. In ultrahigh purity O_2, the peak mobility appears at 2.39 $cm^2/V{\cdot}s$ (figure 5 a)) at H_2O concentrations of 15 - 100 ppb. Then, the peak shifts to 2.31 $cm^2/V{\cdot}s$ at H_2O concentrations of 3900 ppb (figure 5 b)). At H_2O concentrations of 4600 ppb, two peaks appear at 2.31 and 2.21 $cm^2/V{\cdot}s$ (Figure 5 c)), although the average mobility was 2.27 $cm^2/V{\cdot}s$ as shown in figure 4. The peak mobility is 2.21 $cm^2/V{\cdot}s$ in Figures 5 d) – 5 f) and an additional peak appears at 2.15 $cm^2/V{\cdot}s$ in Figures 5 e) and 5 f). These variations in the negative ion mobility indicated that the ion species changed in accordance with the following reactions as the H_2O concentration increased.

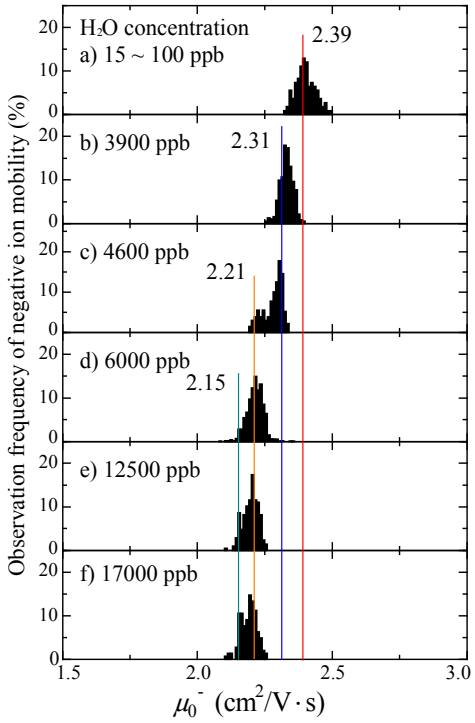

Figure 5 Mobility histogram

$$e + O_2 + O_2 \rightarrow O_2^- + O_2 \quad (1)$$
$$O_2^- + O_2 + O_2 \rightarrow O_4^- + O_2 \quad (2)$$
$$O_2^- + H_2O + O_2 \rightarrow O_2^-{\cdot}(H_2O) + O_2 \quad (3)$$
$$O_4^- + H_2O \rightarrow O_2^-{\cdot}(H_2O) + O_2 \quad (4)$$
$$O_2^-{\cdot}(H_2O)_n + H_2O + O_2 \rightarrow O_2^-{\cdot}(H_2O)_{n+1} + O_2 \ (n \geq 1) \quad (5)$$

The mobility of 2.39 $cm^2/V{\cdot}s$ is considered to be that of O_4^- as described above. The main reason for the shift in the peak mobility from 2.31 to 2.15 $cm^2/V{\cdot}s$ is considered to be the occurrence of reaction (5). The mobility of 2.15 $cm^2/V{\cdot}s$ is in good agreement with that of 2.16 $cm^2/V{\cdot}s$ for O_2^- reported by Snuggs et al. [4], which was measured at low pressures of 0.02 to 10 Torr. However, we measured the negative ion mobility at atmospheric pressure.

4. Conclusion

The mobility of negative ions was measured in O_2 while varying the H_2O concentration. A constant mobility of 2.39 $cm^2/V{\cdot}s$ attributed to that of O_4^- was observed in reduced electric fields of $3 \times 10^{-2} \leq E/N \leq 4.5$ Td at H_2O concentrations of 15 - 100 ppb. With increasing H_2O concentration, mobilities of 2.31 and 2.21 $cm^2/V{\cdot}s$ were observed in H_2O concentration ranges of 3500 - 4600 and 4600 - 17000 ppb, respectively, which were considered to be those of $O_2^-{\cdot}(H_2O)_n$.

5. References

[1] E. A. Mason and E. W. McDaniel, TRANSPORT PROPERTIES OF IONS IN GASES, *John Wily and Sons, Inc., New York* (1988)

[2] H. W. Ellis, R. Y. Pai and E. W. McDaniel, *ATOMIC DATA AND NUCLEAR DATA TABLES* **17** (1976) 177

[3] private communication, www.lxcat.net (2015)

[4] R. M. Snuggs, J. H. Schummers, D. W. Martin, E. W. McDaniel and D. J. Volz, *Phys. Rev. A*, **3** (1971) 477

[5] L. G. McKnight, *Phys. Rev. A*, **2** (1970) 763

[6] L. Harrison and J. L. Moruzzi, *J. Phys. D* **5** (1972) 1239

[7] J. de Urquijo, A. Bekstein, O. Ducasse, G. Ruiz − Vargas, M. Yousfi and M. Benhenni, *Eur. Phys. J. D* **55** (2009) 637

[8] M. Sabo, J. Páleník, M. Kučera, H. Han, H. Wang, Y. Chu, Š. Matejčík, *Int. J. Mass Spectrum.* **293** (2010) 23

[9] R.G. Ewing, D.A. Atkinson, G.A. Eiceman, G.J. Ewing, *Talanta* **54** (2001) 515

[10] M. Sabo, M. Malásková and Š. Matejčík, *Analyst* **139** (2014) 5112

[11] T. Keller, A. Schneider, E. Tutsch-Bauer, J. Jaspers, R. Aderjan and G. Skopp, *IJIMS* **2** (1999) 22

[12] Y. Okuyama, S. Suzuki, H. Itoh, *The XXII Europhysics Conference on Atomic and Molecular Physics of Ionized Gases* (2014) P3-02-01

[13] Y. Okuyama, S. Suzuki, H. Itoh, *IEEJ Trans. FM* **133** (2013) 578 (in Japanese)

[14] Y. Okuyama, T. Kimura, S. Suzuki and H. Itoh, *J. Phys. D* **45** (2012) 195202

[15] H. Abe and H. Kitano, *Sens. Actuators A*, **128** (2006) 202

[16] H. Abe and K. Yamada, *Sens. Actuators A*, **165** (2011) 230